Spectroscopy of ^{7}He using the ^{9}Be(^{6}He ,^{8}Be) transfer reaction

F. Renzi,[1,*] R. Raabe,[1] G. Randisi,[1] D. Smirnov,[1,†] C. Angulo,[2,‡] J. Cabrera,[2] E. Casarejos,[2,§] Th. Keutgen,[2] A. Ninane,[2] J. L. Charvet,[3] A. Gillibert,[3] V. Lapoux,[3] L. Nalpas,[3] A. Obertelli,[3] F. Skaza,[3] J. L. Sida,[3] N. A. Orr,[4] S. I. Sidorchuk,[5] R. Wolski,[5,6] M. J. G. Borge,[7] and D. Escrig[7,‖]

[1]*KU Leuven, Department of Physics and Astronomy, Instituut voor Kern- en Stralingsfysica, Celestijnenlaan 200D, 3001 Leuven, Belgium*

[2]*Centre de Recherches du Cyclotron, Université Catholique de Louvain, B-1348, Louvain-la-Neuve, Belgium*

[3]*CEA-Saclay, DRF/IRFU/SPhN, F-91191, Gif-sur-Yvette Cedex, France*

[4]*LPC-Caen, ENSICAEN, IN2P3/CNRS, Normandie Université, 14050, Caen Cedex, France*

[5]*Flerov Laboratory of Nuclear Reactions, JINR, RU-141980, Dubna, Russia*

[6]*Institute of Nuclear Physics, PAN, PL-31342, Crakow, Poland*

[7]*Instituto de Estructura de la Materia, CSIC, E-28040, Madrid, Spain*

(Received 8 June 2016; published 29 August 2016)

The unbound nucleus ^{7}He has been investigated via the reaction of a 16.8 MeV ^{6}He radioactive ion beam on a ^{9}Be target. The measurement of the outgoing ^{8}Be through its well characterized two-α decay permitted the energy of the ^{6}He $+n$ system to be reconstructed. Through comparison with a complete Monte Carlo simulation incorporating R-matrix lineshapes, the ^{7}He ground state was determined to lie 0.380(28) MeV above the neutron decay with a width of $\Gamma = 0.179(21)$ MeV. A neutron spectroscopic factor SF $= 0.608(18)$ was extracted in agreement with the most recent calculations. Significant evidence was found for a broad resonance lying at 2.6(2) MeV above threshold with a $\Gamma_{\mathrm{FWHM}} = 2.3(3)$ MeV. These parameters are fully consistent with the properties of $1/2^{-}$ state reported by Wuosmaa *et al.* [Phys. Rev. C **72**, 061301(R) (2005)]. Limits were also put on the presence of narrow resonances seen in earlier experiments.

DOI: 10.1103/PhysRevC.94.024619

I. INTRODUCTION

The study of light nuclei far from stability provides crucial constraints for different nuclear structure theories. Particularly, the extreme N/Z ratio characteristic of the very light nuclei makes them suitable for testing *ab inito* approaches, which have achieved remarkable progress in the description of light unbound states.

Since its first observation, the unbound ^{7}He nucleus has been the focus of numerous works. Its ground state was identified in the ^{7}Li(t,^{3}He) charge-exchange reaction [1,2] as a $J^{\pi} = 3/2^{-}$ resonance with a width of 0.16(3) MeV (full width at half maximum; FWHM) at 0.44(3) MeV above the ^{6}He $+n$ threshold. This observation was further confirmed by other experiments [3–10], although quantitative values slightly differ, as shown in Fig. 1. For many years, despite the several attempts (see Ref. [22] for a review), no excited state was found. Korsheninnikov *et al.* [13] were the first to identified an excited state in ^{7}He. They investigated the p(^{8}He ,d)^{7}He reaction at 50 MeV/nucleon observing a resonance at 2.9(3) MeV, with a width $\Gamma = 2.2(3)$ MeV. As decay proceeds mainly into $\alpha + 3n$, the state was interpreted as a $p_{3/2}$ neutron coupled to the unbound 2^{+} excited state of ^{6}He, leading to a tentative spin-parity assignment $J^{\pi} = 5/2^{-}$. Three other experiments showed a resonance with an excitation energy in good agreement with Ref. [13]: the ^{9}Be(^{15}N ,^{17}F)^{7}He transfer reaction [3], ^{8}He(p,d)^{7}He at 15.6 MeV/nucleon [6] and (d,^{3}He) reaction with ^{8}Li beam of 76 MeV [12]. In the latter two measurements the decay of the ^{7}He $5/2^{-}$ state into $\alpha + 3n$ was also confirmed.

In the standard shell-model prediction ^{7}He ground state corresponds to a neutron in the $1p_{3/2}$ orbital coupled with ^{6}He ground state; however, as reported in Table I, the spectroscopic factors from recent calculations agree on the importance of other configurations which are built on ^{6}He(2^{+}). The latter ^{6}He(2^{+}) configuration also plays a crucial role in the wave function of ^{7}He $5/2^{-}$ state [20,23,24].

Most models predict $J^{\pi} = 1/2^{-}$ for the first-excited state of ^{7}He (see Fig. 1). According to Table I, the predominant configuration consists of a $p_{1/2}$ neutron coupled to the ^{6}He ground state. In a shell-model framework this state is the spin-orbit partner of ^{7}He$_{\mathrm{g.s.}}$ and it plays an important role in understanding the spin-orbit interaction in the light neutron-rich dripline nuclei. The promotion of a nucleon from the $p_{3/2}$ to the $p_{1/2}$ orbital causes an excited state above 2 MeV, in the known cases of ^{9}Be, ^{9}B, ^{9}Li, ^{9}C, ^{11}C, and ^{11}B [22,26]. However, for the ^{7}He nucleus experimental results on the properties of $1/2^{-}$ state are still controversial and uncertain.

Two independent measurements found a narrow and low-lying excited state. Meister *et al.* [4] studied ^{7}He with a beam of 227 MeV/nucleon ^{8}He on a carbon target. Selecting the one-neutron-knockout channel, they observed a clear deviation of the ^{6}He $+n$ invariant mass spectrum from the expected R-matrix lineshape. Their result was interpreted as the ^{7}He ground state in addition to a low-lying $J^{\pi} = 1/2^{-}$ state at

*francesca.renzi@fys.kuleuven.be

†Present address: Atys Concept, F-33210 Arcachon, France.

‡Present address: Tractebel Engineering S.A., Avenue Ariane 7, B-1200 Brussels, Belgium.

§Present address: Universidade de Vigo, E-36310 Vigo, Spain.

‖Present address: Consejo de Seguridad Nuclear, c/Justo Dorado, 11 E-28040 Madrid, Spain.

TABLE I. Spectroscopic factors (SF) from complex scaling method (CSM) [20], variational Monte Carlo (VMC) [25],[a] and no core shell model (NCSM) [24] calculations. For CSM calculations only the real part of the values are reported.

^{7}He	^{6}He-$n(lj)$	CSM	VMC	NCSM[b]
$3/2^-$	0^+-$p_{3/2}$	0.64	0.565[c]	0.56
	2^+_1-$p_{1/2}$	0.005	0.006	0.001
	2^+_1-$p_{3/2}$	1.54	2.02	1.97
$1/2^-$	0^+-$p_{1/2}$	1.00	0.91	0.94
	2^+_1-$p_{3/2}$	0.10	0.26	0.34
$5/2^-$	2^+_1-$p_{1/2}$	0.85	0.81	0.77
	2^+_1-$p_{3/2}$	0.10	0.37	0.49

[a]The numerical values for spectroscopic factors in the VMC model are taken from Ref. [24].
[b]In Ref. [24] the authors underlined that the obtained SFs were an intermediate step to use as input for no-core shell model with continuum (NCSMC) calculations, not the aim of their work.
[c]Green's function Monte Carlo (GFMC) result, while the VMC calculation gave a SF equals 0.53; see Ref. [25].

0.6(1) MeV with a width $\Gamma = 0.75(8)$ MeV. The detection of the ^{6}He nucleus excludes this state as the $5/2^-$ state observed in Ref. [13]. In the work of Skaza *et al.* [6], the excitation energy spectrum of ^{7}He was described by assuming a resonance at 0.9(5) MeV ($\Gamma = 1.0(9)$ MeV). The analysis of the (p,d) transfer to this state and its decay in ^{6}He $+n$ were consistent with $1/2^-$ assignment. Recently, Aksyutina *et al.* [9] carried out an almost identical experiment to that reported in Ref. [4], replacing the carbon target by a liquid-hydrogen target; the low-lying resonance was not confirmed. Furthermore, no evidence for a state below 1 MeV has been found in five other experiments [5,11,12,14,15] using a variety of techniques. These studies have provided positive signs of a first-excited state at higher energy, although these observations are not completely in agreement among themselves, as shown in Fig. 1.

We report the results of a new measurement, performed by using the ^{9}Be(^{6}He,^{7}He)^{8}Be reaction. This reaction is characterized by very clear identification of the channel of interest due to the ^{8}Be decay. Indeed, the ground state of ^{8}Be decays exclusively into two α particles with a very small breakup energy ($Q = 0.092$ MeV). For kinetic energies of ^{8}Be above some hundreds of keV, the two α particles remain kinematically focused and can be identified by coincident detection in a charged-particle detector. The effectiveness of this identification technique by ^{8}Be decay have been described in detail by Wozniak *et al.* [27–29], and it has been successfully confirmed in experimental studies with both stable and radioactive ion beams [30,31]. In the present measurement,

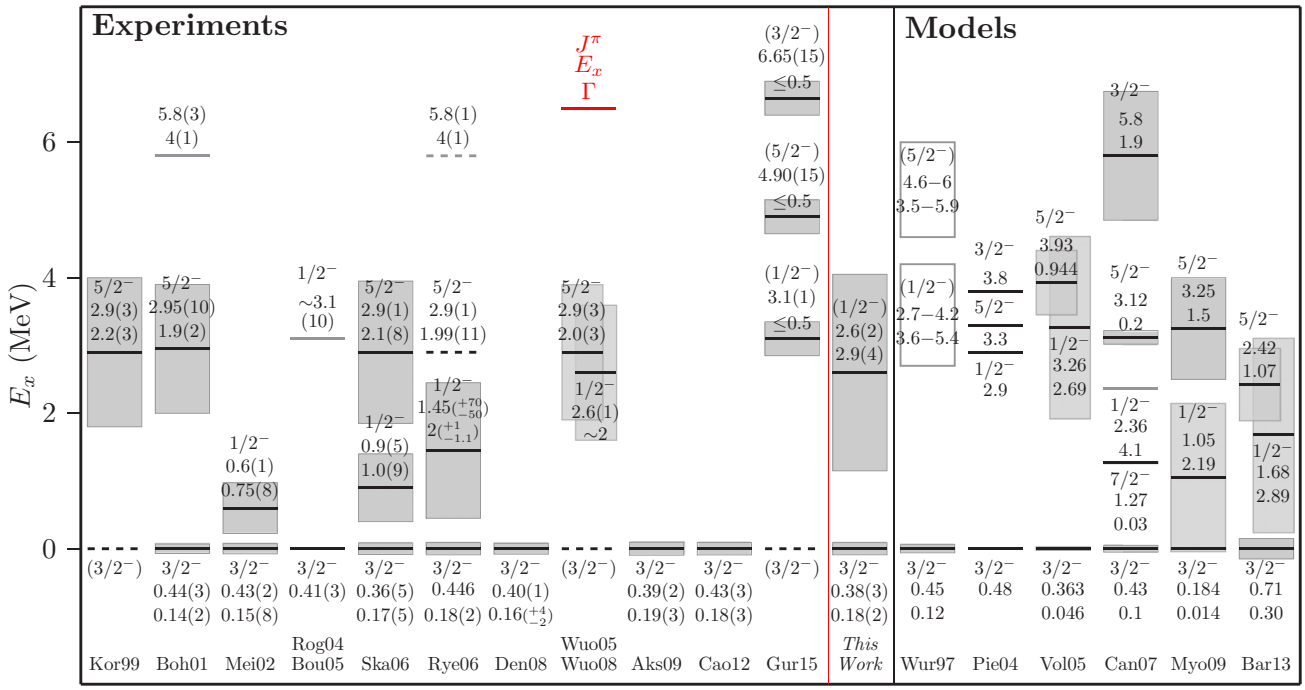

FIG. 1. Summary of the most recent results for the ^{7}He nucleus from experiments, on the left, and from theoretical calculations, on the right. The solid lines represent the energy of the states in ^{7}He, the shaded bands correspond to the widths (Refs. [11,12] quoted the FWHM). When the width is too broad to be drawn a solid gray line is used. Dashed lines indicate that the resonance parameters are taken from the literature. The energy values for ^{7}He$_{g.s.}$ are given with respect to the ^{6}He $+n$ threshold. The results of the present work are included for a side-by-side comparison. On the bottom, the symbolic references to the previous results indicate, in order, the work of Korsheninnikov *et al.* (Kor99: [13]), Bohlen *et al.* (Boh01: [3]), Meister *et al.* (Mei02: [4]), Rogachev *et al.* (Rog04: [5]), Boutachkov *et al.* (Bou05: [14]), Skaza *et al.* (Ska06: [6]), Ryezayeva *et al.* (Rye06: [7]), Denby *et al.* (Den08: [8]), Wuosmaa *et al.* (Wuo05: [11] and Wuo08: [12]), Aksyutina *et al.* (Aks09: [9]), Cao *et al.* (Cao12: [10]), Gurov *et al.* (Gur15: [15]), Wurzer and Hofmann (Wur97: [16]), Pieper *et al.* (Pie04: [17]), Volya and Zelevinsky (Vol05: [18]), Canton *et al.* (Can07: [19]), Myo *et al.* (Myo09: [20]), and Baroni *et al.* (Bar13: [21]).

from the position and energy of coincident α particles, the reaction $^{9}\mathrm{Be} + {}^{6}\mathrm{He} \rightarrow \mathrm{X} + {}^{8}\mathrm{Be} \rightarrow \mathrm{X} + \alpha + \alpha$ is reconstructed with the resonant particle spectroscopy technique [32]. Then, the center-of-mass energy of the undetected system X is obtained.

The ^{7}He states can be populated via both one-neutron and two-proton pickup from the ^{9}Be target. Because of the small neutron separation energy of ^{9}Be ($S_n = 1.665$ MeV), the former reaction mechanism, (^{6}He ,^{7}He), can be considered a direct reaction. Therefore, it is expected that one-neutron pickup would selectively populate states containing the ^{6}He ground-state configuration; namely, the ^{7}He $3/2^-$ ground state and $1/2^-$ excited state (see Table I). In addition, when ^{8}Be are measured at forward angles relative to the beam direction, the two-proton pickup mechanism may contribute significantly. In fact, Milin at al. [31] showed that the (^{6}He ,^{8}Be) reaction proceeds via direct process even at incident energies around 3 MeV/nucleon, resulting in a relatively high cross section, mainly because of the overlap between the ^{6}He and ^{8}Be wave functions [31]. However, only the ^{7}He ground state is expected to be directly populated via the pickup of two-protons from the ^{9}Be target, whereas excited states of ^{7}He involving excitations in the neutron configuration require higher-order processes.

This paper is organized as follows: In Sec. II the employed detection systems and the measurement are described. In Sec. III the analysis method is explained in detail and the results are presented. Finally, Sec. IV is dedicated to the discussion of the results and a summary is given in Sec. V.

II. MEASUREMENT

The experiment was performed at the Cyclotron Research Center (CRC) in Louvain-la-Neuve, Belgium [33]. The ^{6}He beam was produced by the isotope-separation-on-line (ISOL) technique using two coupled cyclotrons, CYCLONE30 and CYCLONE110 [34]. An intense proton beam (200 μA) delivered by CYCLONE30 impinged on a LiF target, where the ^{6}He nuclei were produced via $^{7}\mathrm{Li}(p,2p)^{6}\mathrm{He}$ reaction. The nuclei diffused out of the target and were collected and ionized in an electron-cyclotron resonance (ECR) ion source. They were then injected and accelerated in CYCLONE110, which was tuned to operate as a powerful mass spectrometer: no evidence of the ^{6}Li isobaric contaminant was seen during the measurement. The final $^{6}\mathrm{He}^{+}$ beam had an energy of $E_{\mathrm{lab}} = 16.8$ MeV and an average intensity on target of about 10^{7} particles per second (pps) for three days of measurement. To verify the reliability of the detection method, a ^{6}Li beam at $E_{\mathrm{lab}} = 17$ MeV was used to measure the $^{6}\mathrm{Li}(^{9}\mathrm{Be}\,,^{8}\mathrm{Be})^{7}\mathrm{Li}$ reaction. The intensity of this beam was above 10^{7} pps for about 10 hours of irradiation.

The target was a 400-μg/cm^2-thick self-supporting foil of ^{9}Be produced at the Laboratori Nazionali del Sud in Catania, Italy. This was mounted on a target ladder, together with a 200-μg/cm^2-thick Au target used for calibration. As shown in Fig. 2, the detection setup consisted of two annular single-sided silicon detector arrays (SSD) [35]: LEDA (Louvain–Edinburgh detector array) and Lamp, named after its shape. These were composed of eight and six SSD sectors, respectively. Lamp sectors are tilted at 45 degrees with respect

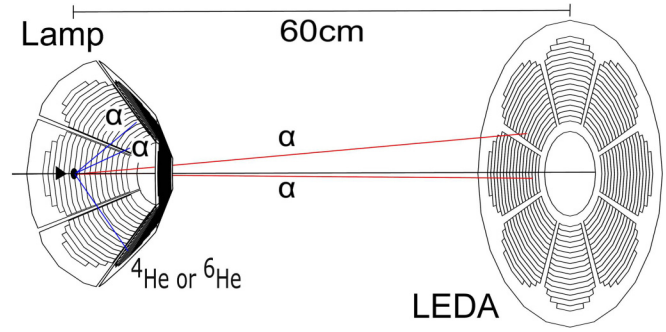

FIG. 2. Schematic drawing of the experimental setup. On the left side of the figure, the arrow shows the beam direction and the back disk in front of Lamp is the target. The Faraday cup, placed behind LEDA, is not drawn.

to the beam direction. Each sector has 16 strips (5 mm strip pitch), in total the setup had 224 detection channels over the full azimuthal range. LEDA was placed about 60 cm from the target, covering polar angles between 5 and 12 degrees in the laboratory frame, whereas Lamp was set closer to detect particles in a polar angular range of 22–71 degrees. Therefore, the setup provided a high angular coverage in the forward hemisphere, combined with high segmentation at small laboratory angles. Additional information on the experimental setup can be found in Ref. [36].

The energy and time of flight (with respect to the cyclotron radio frequency) of all charged particles hitting the detectors were recorded. The intrinsic energy resolution of the Si strip was about 25 keV FWHM (for 5.486 MeV α particles). The convolution of the time resolution of the Si detector and the cyclotron radio frequency was about 4 ns FWHM, while, for instance, the time of flight from the target to LEDA was around 30 ns for 8 MeV α particles. In LEDA the particle identification was achieved by the time-of-flight method, because the mass resolution permitted us to clearly distinguish ^{4}He from ^{6}He particles, as evident from Fig. 3. In contrast, for Lamp the small distance to the target and the larger solid angle of each strip, consequence of the tilted sectors, resulted in a poor mass

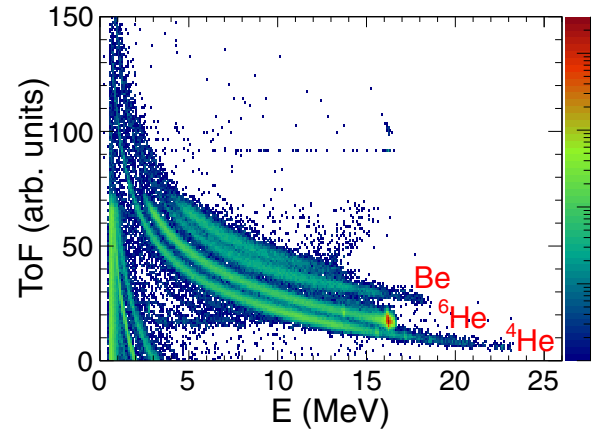

FIG. 3. The time of flight (ToF) versus the energy for one strip of the LEDA array. For explanations, see Ref. [36].

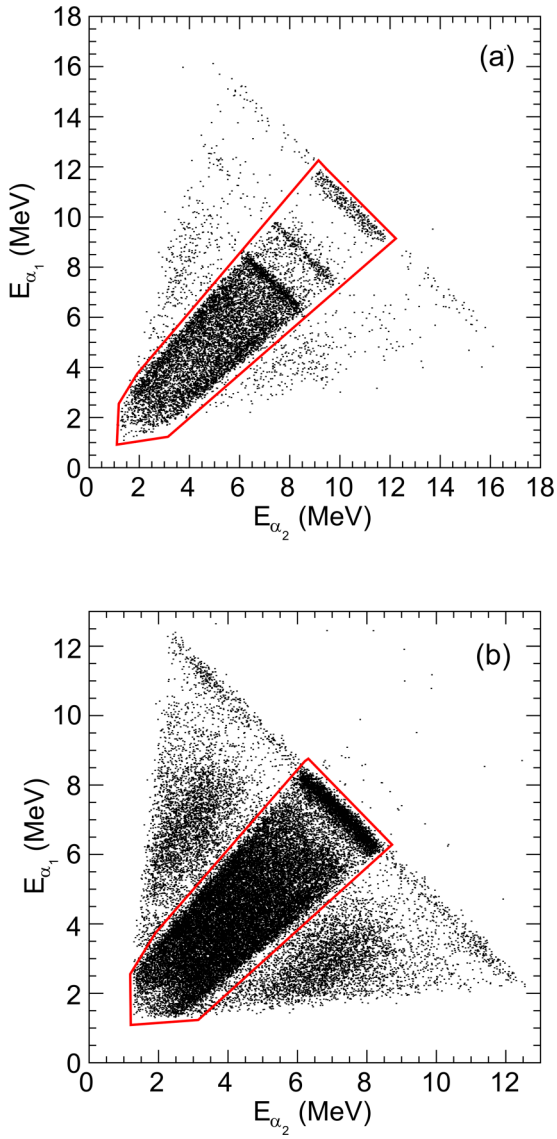

FIG. 4. The two-dimensional energy spectra E_{α_1}-E_{α_2} for events (a) with two α particles in coincidence in LEDA, in the case of ^{6}Li beam, and (b) when the beam is ^{6}He. The contours (gates) indicated in the plots are discussed in the text.

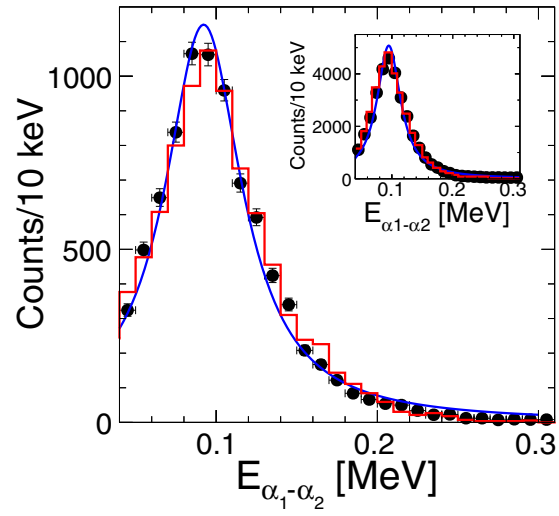

FIG. 5. The reconstructed relative energy of the two α particles, both detected in LEDA, in the case of ^{6}Li beam (result for ^{6}He beam in the inset); the gate on ^{8}Be$_{\text{g.s.}}$ is applied. According to the Breit–Wigner function fit, shown as solid line, the peak lies at 92.2(4) keV with a width $\Gamma_{\text{FWHM}} = 58(1)$ keV. The histogram is the result of the simulation described in the text.

separation. In this case the identification of α particles from the ^{8}Be$_{\text{g.s.}}$ decay only relied upon the kinematic reconstruction.

Determination of the beam dose was performed from the direct beam current measurement on a Faraday cup placed behind the detection setup. The correct normalization of this reading was obtained by measuring the elastic scattering of ^{6}He on the Au target.

Figure 4 shows two-dimensional energy spectra E_{α_1} versus E_{α_2} when two α particles were detected in coincidence in LEDA, for the ^{6}Li and ^{6}He beams. The plots present two patterns, perpendicular to and around the diagonal $E_{\alpha_1} = E_{\alpha_2}$. The former corresponds to kinematic loci of constant total energy, hence to definite states of final nuclei; the latter is given by the events with the same relative energy between two α particles, thus related to the ^{8}Be excitation energy. Events with two α particles from the ^{8}Be$_{\text{g.s.}}$ decay, which is the signature for the reaction of interest, were selected with the solid line gate, shown in Fig. 4. The reliability of this selection can be verified by performing the kinematical reconstruction. From the energies, the scattering angles θ and azimuthal angles ϕ of each particle (given by the positions of the strips and sectors, respectively), the relative energies of the system α-α in its own center of mass is calculated and displayed in Fig. 5. The peak corresponds to the decay of the ^{8}Be ground state ($Q =$ 0.092 MeV). Its width is much larger than the intrinsic one, 5.57(0.25) eV [22], because it is dominated by experimental factors (mainly uncertainties on the angles).

The two α particles are confined within a breakup cone. The edges of the cone are defined by the maximum half break angle, $\beta_{\text{max}} = \arcsin\{[(0.092\ \text{MeV})/E(^8\text{Be})]^{1/2}\}$ [28], where $E(^8\text{Be})$ is the kinetic energy of the ^{8}Be and 0.092 MeV is the Q value of the decay assuming the ^{8}Be in its ground state. In Fig. 6 the values of β_{max} in function of the ^{8}Be kinetic energy are compared with the half of the relative angle between the two α particles, as obtained from the polar and azimuthal observed angles, $\theta_{12}/2 = [\cos\theta_1 \cos\theta_2 + \sin\theta_1 \sin\theta_2 \cos(\phi_1 - \phi_2)]/2$ [37]. The maximum half-cone size of 8 degrees proves the kinematic focusing of the two particles and their spatial correlation.

The energies and angles of the detected α particles from the ^{8}Be$_{\text{g.s.}}$ decay were used to reconstruct the center-of-mass energy of ^{6}He $+n$ system. Assuming a three-body final state $^9\text{Be} + {}^6\text{He} \rightarrow \text{X} + {}^8\text{Be} \rightarrow \text{X} + \alpha + \alpha$, the three-body Q value, Q_3, is calculated from momentum and energy conservation [32,37]. If Q_{ggg} is the Q value when all the three final particles are in their ground states, the difference between Q_{ggg} and the calculated Q_3 provided the excitation energy spectrum of the undetected system, which is $^6\text{He} + n$

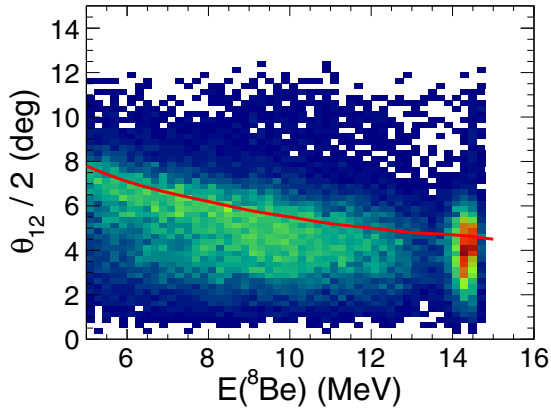

FIG. 6. Half of the angle between the two α particles versus the calculated kinetic energy of ^{8}Be nucleus. The line defines the maximum half break angle, β_{max}, as described in the text.

in the present case. All the spectra are calculated as function of the resonance energy above the neutron threshold. An identical reconstruction has been applied for the excitation energy spectrum of ^{7}Li, which is shown in Fig. 7, when the two α particles from the ^{8}Be$_{g.s.}$ decay are both detected in LEDA. The center-of-mass energy of ^{6}He + n system from the LEDA and Lamp data are presented in Figs. 8 and in 9, respectively. For the latter spectrum, three charged-particle coincident events were selected: two α particles from ^{8}Be$_{g.s.}$ decay and a ^{4}He or a ^{6}He in the opposite Lamp sector, as schematically drawn in Fig. 2. Due to the kinematics, an equivalent condition could not be set by using the LEDA data. The energy loss of the α particles in the target has to be accounted for in the calculations above. Since the reaction point is not known, the energy loss was calculated for half the thickness of the target including a

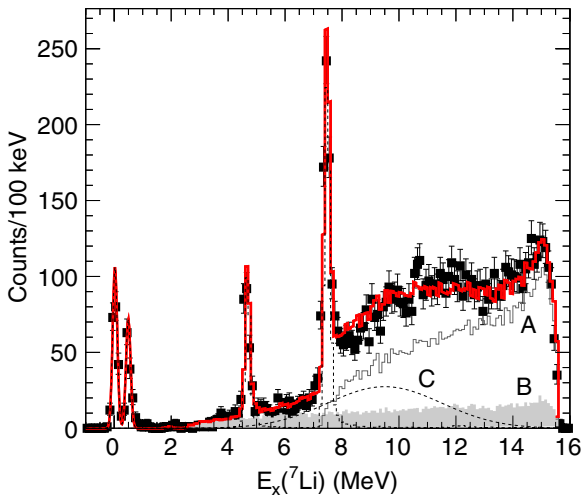

FIG. 7. The excitation energy spectrum for ^{7}Li selecting events with α particles from ^{8}Be$_{g.s.}$ decay in LEDA. The thick solid red line is the total fit including the contributions due to the populated states (dashed lines and curve C) and the three-body phase-space background: ^{6}Li + ^{9}Be $\rightarrow$ ^{6}Li + n + ^{8}Be (curve A) and ^{6}Li + ^{9}Be $\rightarrow$ ^{4}He + ^{3}H + ^{8}Be (curve B).

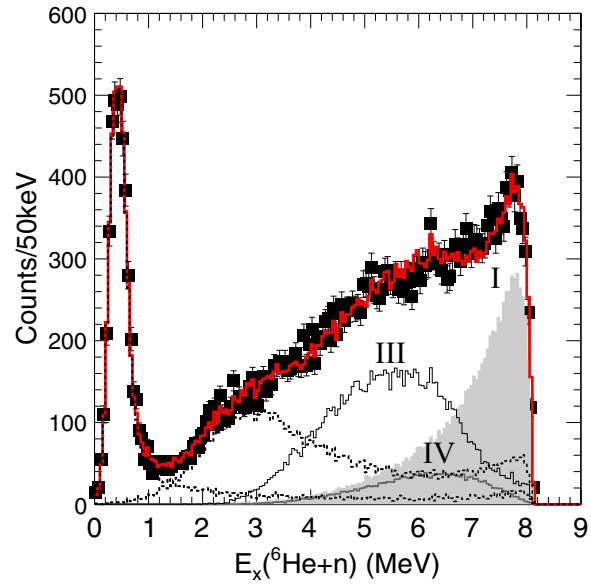

FIG. 8. The center-of-mass energy of ^{6}He + n system, obtained by selecting events with α particles from ^{8}Be$_{g.s.}$ decay in LEDA. The thick solid red line is the total fit including the contributions due to the populated states in ^{7}He (dashed lines), the five-body phase-space background ^{6}He + ^{9}Be $\rightarrow$ ^{4}He + n + n + n + ^{8}Be (curve I), direct decays of ^{10}Be* and ^{11}Be* (curves III and IV, respectively). The fit reduces the three-body phase-space contribution, ^{6}He + ^{9}Be $\rightarrow$ ^{6}He + n + ^{8}Be, to a value in agreement with zero.

correction for the scattering angles. Tables obtained with the program SRIM [38] were used.

III. ANALYSIS AND RESULTS

The spectra of ^{9}Be + ^{6}He $\rightarrow$ X + ^{8}Be$_{g.s.}$ (^{9}Be + ^{6}Li $\rightarrow$ X + ^{8}Be$_{g.s.}$) reaction include two types of contributions: peaks related to populated states of ^{7}He (^{7}Li) and events from other channels with ^{8}Be$_{g.s.}$ as a final nucleus. The latter ones constitute our background, which we need to carefully evaluate in order to extract the properties of the populated states in ^{7}He (^{7}Li). To describe these contributions we adopted an analysis method similar to that used by Denby *et al.* [8]. We developed an extensive Monte Carlo simulation including all processes leading potentially to ^{8}Be$_{g.s.}$. The simulated data are then analyzed with the same procedure of the measured data. Our Monte Carlo package was GEANT4 based [39] and it included an accurate description of the beam features, the reaction mechanism, and the experimental setup. First, the GEANT4 code tracks ^{6}He (^{6}Li) beam particles in the ^{9}Be target, simulating the energy loss and the straggling until a random point of interaction, where the reaction is generated. The resulting particles are then propagated through the detection setup and the energies deposited in the detector material is recorded. The reaction processes used to simulate our background are discussed in the following sections.

When resonances are involved in the simulated reaction, their lineshapes were considered as input in the generation part of the Monte Carlo package. These were parametrized by using a single-level R-matrix code. As detailed in Refs. [40,41], in a

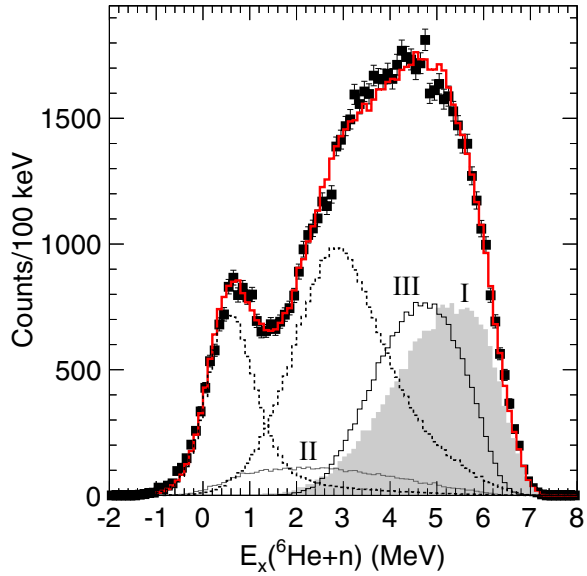

FIG. 9. The center-of-mass energy of the ^{6}He $+n$ system, obtained by selecting events with α particles from the ^{8}Be$_{g.s.}$ decay in Lamp. The thick solid red line is the total fit including the contributions due to the populated states (dashed lines), the five-body phase-space background ^{6}He $+^9$Be $\rightarrow$ ^{4}He $+n+n+n+^8$Be (curve I), the three-body phase-space background ^{6}He $+^9$Be $\rightarrow$ ^{6}He $+n+^8$Be (curve II), and the direct decays of ^{10}Be* (curve III).

single-level approximation a resonance of an unbound system $C+n$, for instance ^{6}He $+n$, is described as

$$\frac{d\sigma}{dE_{Cn}} \propto \frac{\Gamma_\ell(E_{Cn})}{[E_r+\Delta_\ell(E_{Cn})-E_{Cn}]^2+\frac{1}{4}\Gamma_\ell^2(E_{Cn})}, \quad (1)$$

where E_{Cn} is the relative energy of the system $C+n$ in its own center of mass and E_r is the resonance energy, $\Delta_\ell(E_{Cn})$ is the resonance shift, $\Gamma_\ell(E_{Cn})=2\gamma^2 p_\ell(E_{Cn})$ with γ^2 the reduced width and $p_\ell(E_{Cn})$ the penetrability function ℓ is the relative angular momentum between C and n.

The theoretical lineshapes for the resonances of ^{8}Be, ^{7}Li were calculated with R-matrix code by using energies and widths of the states taken from the literature [22] and channel radius R equals 4.5 fm for ^{8}Be [42], and $R=r_0(A_f^{1/3}+A_n^{1/3})$ with r_0 set at 1.40 fm for ^{7}Li. The value $r_0=1.41$ fm was utilized for ^{7}He resonances. For ^{7}He, however, the energies and the widths were varied over a large range of values. For each set of resonance parameters a Monte Carlo simulation was carried out and the results were used, together with the simulated background, to fit the experimental energy spectra. In the fit, the normalization factor of each contribution was taken as a free parameter. By iterating the simulation and the fit for a large number of energies and widths of the ^{7}He resonances, a χ^2 surface was obtained, from which energies, widths, and their uncertainties were estimated.

In both ^{7}Li and ^{7}He cases, the fit of energy spectra was performed by using a minimum number of resonances. The consistent agreement between the experimental and simulated data was verified in each step of the reconstruction process. For instance, Fig. 5 shows the energy in the center of mass of two α particles detected in LEDA, when the selection illustrated in Fig. 4 is applied. The ground state of ^{8}Be is found at the right energy, and its width, entirely due to experimental factors, is well reproduced by the simulation.

TABLE II. The low-lying energy levels of ^{7}Li from the TUNL Nuclear Data Group (NDG) evaluation [43].

E_x (MeV $\pm$ keV)	$J^\pi;T$	τ_m or $\Gamma_{c.m.}$ (keV)	Decay
g.s.	$3/2_1^-;1/2$		Stable
0.478 ± 0.003	$1/2_1^-;1/2$	$\tau_m=105\pm3$ fs	γ
4.652	$7/2_1^-;1/2$	$\Gamma_{c.m.}=69$ keV	t,α
6.604	$5/2_1^-;1/2$	918	t,α
7.454	$5/2_2^-;1/2$	80	n,t,α
8.75	$3/2_2^-;1/2$	4712	n,α
9.09	$1/2_2^-;1/2$	2752	n,t,α
9.57	$7/2_2^-;1/2$	437	n,t,α

A. Analysis of ^{7}Li spectrum

The method presented above was first applied to describe the ^{7}Li excitation spectrum, as a validation of the analysis procedure. For this reason, the R-matrix lineshapes for the ^{7}Li resonances were calculated with energies and widths from the known states listed in Table II. In the ^{7}Li excitation energy spectrum, Fig. 7, four peaks are firmly resolved. The peaks correspond to the ^{7}Li ground state, the $1/2_1^-$ bound state, and the $7/2_1^-$ and $5/2_2^-$ unbound states.

The $5/2_1^-$ state at $E_x=6.604$ MeV ($\Gamma=918$ keV) is not clearly observed. In Ref. [44] the authors argue that the wave function of $5/2_1^-$ state has no fractional parentage with the predominant term in the ^{6}Li$_{g.s.}$ wave function. This and the large width of the state would explain the missing identification in the present measurement.

The reactions involving the ^{7}Li resonances were simulated by using precisely the energies and widths values reported in Table II for the R-matrix calculation. Conversely, the ground state and the first-excited state are bound, thus do not require R-matrix parametrization in the GEANT4 code; the excitation energy of the first-excited state was set at 0.478 MeV as given in Table II. The simulation output for these bound states were two Gaussian distributions.

The experimental resolution was 0.19 MeV FWHM. This rather good value is an effect of a peculiar similarity between the energy loss in the target by the ^{6}Li beam ions and the sum of the two α particles from the ^{8}Be$_{g.s.}$ decay. Consequently, the reconstructed spectrum is less affected by assuming the reaction vertex in the middle of the target. The simulated distributions of the ^{7}Li peaks used in the fit are shown as dashed lines in Fig. 7. It is worth stressing again that the energies and widths used to obtain the simulated distributions are exactly the values reported in Table II. Furthermore, three-body phase-space contributions were considered: ^{6}Li $+^9$Be $\rightarrow$ ^{6}Li $+n+^8$Be (curve A) and ^{6}Li $+^9$Be $\rightarrow$ ^{4}He $+^3$H $+^8$Be (curve B). The amount of these components in the fit is limited by the number of events at high (curve A) and low (curve B) excitation energy. Between 8.5 and 13.0 MeV there are additional events, which could not be described by the

already-mentioned contributions. In the literature [22], three broad resonances are reported in this excitation-energy region (see Table II); however, because of their large widths, the limited experimental evidence and for the sake of simplicity, it seemed appropriate to parametrize these resonances as a single Gaussian-shaped background (curve C). The results of the best fit obtained with these seven components is shown as solid line in Fig. 7 and gives a χ^2 per degree of freedom of 1.74, validating both the reconstruction procedure and the reliability of the analysis method.

B. Analysis of ^{7}He spectra

In the center-of-mass energy of the ^{6}He + n system, Figs. 8 (two α particles from the ^{8}Be$_{g.s.}$ detected in LEDA) and 9 (α particles in Lamp), the peak corresponding to the ^{7}He ground state is fully resolved. However, contrary to the case of the ^{6}Li beam, the ^{6}He beam and the two α particles from ^{8}Be$_{g.s.}$ decay lose significantly different energies in the target. As a consequence, the resolution in the spectrum obtained with the LEDA data is 0.27 MeV FWHM (see Fig. 8). Using Lamp data, Fig. 9, the detector geometry and position induce a large uncertainty on the particle trajectories, so the resolution is 1.1 MeV FWHM. The actual resolution could be estimated by deconvoluting the width of the ^{7}He$_{g.s.}$ (as obtained in the data analysis, see below) from the FWHM of the experimental peaks. In the two figures the ^{7}He ground-state peaks are clearly separated from the rest of the spectrum (higher energy) by a minimum at about 1.5 MeV, which constrains the magnitude of possible background contributions at that energy. However, at higher energy the background might increase because other channels are open.

In earlier experimental studies [3,6,13,45] phase-space contributions played an important role in interpreting the ^{7}He excitation energy spectrum. As for the ^{7}Li spectrum analysis, the few-body components considered here are those with ^{8}Be$_{g.s.}$ as a final nucleus. In the fit we have included the three-body phase space ^{6}He + ^{9}Be $\rightarrow$ ^{6}He + n + ^{8}Be and the five-body phase-space ^{6}He + ^{9}Be $\rightarrow$ ^{4}He + n + n + n + ^{8}Be contributions. Nevertheless, in Fig. 8 the contribution of the three-body phase space is reduced to zero, contrary to the fit of the spectrum obtained with the Lamp data; Fig. 9. As introduced in Sec. I, the mechanism to produce ^{7}He may be different in the angular ranges covered by the two detector arrays. In the range where the one-neutron pickup mechanism is more likely and the 2α particles from the ^{8}Be$_{g.s.}$ decay are detected in Lamp there may be a sizeable contribution of the three-body phase space (^{6}He + ^{9}Be $\rightarrow$ ^{6}He + n + ^{8}Be) to the continuous background. On the other hand, if the 2α particles from the ^{8}Be$_{g.s.}$ decay are detected in LEDA and the the two-proton pickup is the main process, the ^{6}He + n + ^{8}Be channel requires the removal of an additional neutron from the target, possibly suppressing this contribution.

All the simulated distributions of the physical backgrounds are illustrated in Fig. 10. The different shapes, initial rise and the cutoff edges at high excitation energy, corresponding to low-energy α particles, are well consistent with the behavior of both LEDA and Lamp experimental data. Contributions from other channels such as one-neutron and two-neutron

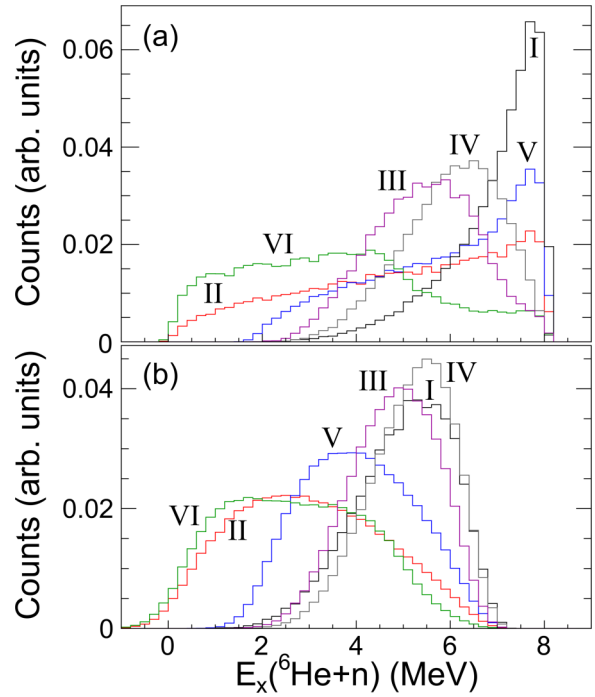

FIG. 10. The simulated physical background in (a) LEDA and (b) Lamp spectra due to ^{6}He + ^{9}Be $\rightarrow$ [I]^{4}He + n + n + n + ^{8}Be; [II] ^{6}He(0$^+$) + n + ^{8}Be; [III] ^{5}He + ^{10}Be*; [IV] ^{4}He + ^{11}Be*; [V] ^{6}He(2$^+$) + n + ^{8}Be; [VI] ^{6}He + ^{9}Be* (J = 1/2$^-$, E_x = 2.78 MeV). The counts are normalized to unity.

stripping reactions were also examined. Results from this same experiment [36] reported the strong population of a ^{11}Be excited state at E_x = 10.6 MeV, higher than the three-neutron emission threshold, which lies at 8.98 MeV [22]. The authors also provided evidence for a sequential population of ^{10}Be excited state at E_x = 9.6 MeV, above the ^{8}Be + 2n threshold situated at 8.48 MeV [22]. We have investigated the contributions in the center-of-mass energy of the ^{6}He + n system due to the direct breakup of this ^{11}Be (^{10}Be) excited state into ^{8}Be + 3n (^{8}Be + 2n). This channel has been simulated by assuming an isotropic emission of ^{8}Be and neutrons in the center of mass. As shown in Fig. 10, the simulation results indicate that the breakup of ^{11}Be (^{10}Be) excited states might contribute mostly in the region of the spectrum above about 3 MeV. In Lamp, the condition of detecting a third charged particle together with the two α particles from ^{8}Be$_{g.s.}$ decay does not kinematically exclude these background contributions. However, their shape can be quite different (see Fig. 10). Contrary to the simulated results for the LEDA array, in Lamp the contribution due to the ^{6}He + ^{9}Be $\rightarrow$ ^{4}He + ^{11}Be* reaction channel has a shape similar to the five-body phase-space background, as a consequence the fit in Fig. 9 reduces to zero the normalization factor of one of these contributions. However, a different relative contribution of this background cannot be ruled out. Other possible sources of background were investigated, such as the three-body phase space ^{6}He + ^{9}Be $\rightarrow$ ^{6}He* + n + ^{8}Be with ^{6}He left in its first-excited state, or the breakup of ^{9}Be* (5/2$^-_1$) and ^{9}Be* (1/2$^-_1$) into n + ^{8}Be$_{g.s.}$. However, their

TABLE III. Parameters for ^{7}He resonances resulting from the best fit of the excitation energy spectra in Figs. 8 and 9. The reported errors are only statistical uncertainties. For the resonance at lower energy, the systematic errors are 7%, 11%, and 11% for E_r, $\Gamma_{\rm FWHM}$, and Γ_ℓ, respectively. For the resonance at higher energy, the systematic errors are 4%, 8%, and 8% for E_r, $\Gamma_{\rm FWHM}$, and Γ_ℓ, respectively. The sources of the systematic errors are discussed in the text. In the last column the SF from previous measurements.

R fm	E_r MeV	$\Gamma_{\rm FWHM}$ MeV	$\Gamma_\ell(E_r)$ MeV	$p_\ell(E_r)$	$\gamma^2_{\rm obs}$ MeV	SF This work[a]	SF Previous works
4	0.380(3)	0.125(2)	0.179(2)	0.098	0.915(20)	0.608(18)	0.512(18) [10] 0.61(3) [9] 0.37(7) [12] 0.64(9) [45]
4	2.600(74)	2.340(70)	2.900(155)	0.914	1.586(120)	1.055(82)	

[a]To calculate the spectroscopic factor (SF) we have used $\gamma^2_{\rm sp} = 1.504(29)$ MeV, as evaluated in Ref. [9].

inclusion did not improve the quality of the fit, so they have been excluded.

Any combination of the background reaction channels described above was not sufficient to correctly reproduce the center-of-mass energy of ^{6}He + n system in the region $E_x = 1.5$ to 5 MeV. For this reason, we added a contribution from an excited state in ^{7}He formed in the ^{6}He + ^{9}Be $\rightarrow$ ^{7}He* + ^{8}Be$_{\rm g.s.}$ process. As previously explained, to determine values and errors of the ^{7}He resonance parameters, more than 60 000 fits were performed to create the χ^2 surface. Each fit included the simulated results of the binary reaction contributions obtained with different R-matrix parametrizations; Eq. (1). Since no information on the ^{7}He decays was used to reconstruct the spectra in Figs. 8 and 9, the parametrization of the resonance shapes by the single-level approximation, Eq. (1), was considered appropriate. For the ^{7}He$_{\rm g.s.}$, E_r has been varied from 0.340 to 0.460 MeV and Γ_ℓ between 0.130 and 0.200 MeV, while for the excited state the investigated ranges were 0.6–4.0 MeV and 0.7–5.0 MeV for E_r and Γ_ℓ, respectively. The variation steps were not constant, but we decreased them in the proximity of the minimum in the χ^2 surface. In all cases, the relative angular momentum ℓ between ^{6}He(0$^+$) and n was set equal to unity. Because the results could be dependent on channel radius R we opted for the value of 4 fm, which has been used in most recent works [9,10,45] and, therefore, permits us to make R-independent comparisons. Due to the significantly better energy resolution achieved with LEDA than with Lamp, the χ^2 surface was only determined by fitting the spectrum from LEDA data. Once the resonance parameters minimizing χ^2 were identified, they were used in the fit of the spectrum from Lamp data.

In Fig. 8 the thick solid line is the result of a fit with simulated contributions that best reproduce the ^{7}He decay energy spectrum from LEDA data, given a $\chi^2 = 171.3$ for 170 degrees of freedom (d.o.f.). The values of the resonance parameters minimizing χ^2 are reported in Table III. The spectroscopic factors for the ^{6}He(0$^+$) + n configuration, SF in the table, are calculated from SF $= \gamma^2_{\rm obs}/\gamma^2_{\rm sp}$, where $\gamma^2_{\rm obs}$ are extracted from the R-matrix parametrization which gives the best fit and $\gamma^2_{\rm sp}$ are the single-particle reduced width. The value assumed for the latter is generally model dependent and this may generate ambiguities when SF from different works are compared. To overcome this problem, the SF is evaluated by considering $\gamma^2_{\rm sp} = 1.504(29)$ MeV as proposed in Ref. [9] and also adopted in Ref. [10]. It should, however, be noted that the reported SF decrease of 25% when the estimation of $\gamma^2_{\rm sp}$ for $\ell = 1$ proposed by Bohr and Mottelson [46] is considered. The SF for the ^{6}He(0$^+$) + n configuration for both the ground state and the excited state of ^{7}He were computed by using the same value for the single-particle reduced width. It is worth noting that the width is sensitive to the spin of the resonance only via the angular momentum ℓ, which is set equal to 1 for the parametrization of both resonances.

The statistical errors are estimated by the $\chi^2 + 1$ statistical analysis method; the systematic uncertainties are due to the energy calibration and to the shifts in detector position, whereas the results are less affected by other sources of systematics, such as variations of target thickness. This has been investigated by modifying inside the nominal errors either the LEDA position or the target thickness in the simulation code. The systematic errors are 25 keV for the position of ^{7}He$_{\rm g.s.}$ and 19 keV for its width; for the position and width of the other resonance they are 100 and 230 keV, respectively. In the Table III the systematic uncertainties for the $\Gamma_{\rm FWHM}$ are derived from the systematic errors of the width and they are 14 and 193 keV.

For the excited state of ^{7}He, the values that minimize the χ^2 are $E_r = 2.6(2)$ MeV and $\Gamma_{\ell=1}(E_r) = 2.9(4)$ MeV, which corresponds to $\Gamma_{\rm FWHM} = 2.3(3)$ MeV. The latter value is intended before the broadening and the effect of the experimental setup, directly from the distribution obtained with the R-matrix code. Although the yield of these resonances are influenced by the definition of the backgrounds, their positions and widths remained stable when attempting the fit with different background combinations. Moreover, no effect on the results due to the binning of the data has been observed. The sign of a second peak is appreciably visible also in Fig. 9. It is worth noting that the good description of both spectra, Figs. 8 and 9, with the same parameters for the two ^{7}He resonances, confirms our interpretation of these data. The difference in the covered angular ranges entails that the processes contribute differently in each spectrum, as evident in the figures.

IV. DISCUSSION

The resonance at $E_r = 380(28)$ keV and $\Gamma_r = 179(21)$ keV is remarkably consistent with the previous observations of the ^{7}He ground state in Refs. [6,9] and good agreement with

the most recent experimental results reported in Fig. 1. As indicated in Table III, four measurements have estimated the neutron spectroscopic factor for the $^6\mathrm{He}(0^+) + n$ configuration in the $^7\mathrm{He}_{\mathrm{g.s.}}$. In the present work, we calculated a SF = 0.608(18), in agreement with the values from the neutron knock-out experiment [9] and with the SF from an R-matrix analysis of $^7\mathrm{Li}(d,^2\mathrm{He})^7\mathrm{He}$ reaction data [45]. A smaller SF has been extracted from the angular distribution study in the proton removal and neutron pickup reactions [11,12]. Although it should be noted that the spectroscopic factors are model-dependent and not pure observables [47], our result is in line with the theoretical prediction in Table I.

To achieve a good description of our spectra, a second ^{7}He resonance has been included in the data fit. Wuosmaa *et al.* [11,12] used complementary reactions, $^8\mathrm{Li}(d,^3\mathrm{He})$ and $^6\mathrm{He}(d,p)$, to selectively populate and probe states with different configurations, $5/2^-$ and $1/2^-$, respectively. The (d,p) reaction data suggested a resonance at 2.6 MeV with a $\Gamma_{\mathrm{FWHM}} \sim 2$ MeV (see Fig. 1), which is in excellent agreement with the present result reported in Table III. In this table, the spectroscopic factor for this resonance is also computed, giving a value comparable with unity. Although this result should be treated with caution due to the vague notion of the spectroscopic factor for the broad resonances in the continuum [48], a comparison with the theoretical calculations in Table I favors the interpretation of observed resonance at 2.6 MeV as the $1/2^-$state. However, in our work, a confirmation of spin of the resonance could not be achieved experimentally. Prior works [4,6,11–13] inferred the spin of the observed ^{7}He excited state, $1/2^-$ or $5/2^-$, through the determination of its decay mode, $^6\mathrm{He} + n$ or $^4\mathrm{He} + 3n$. Here, due to the limited angular resolution of the Lamp detector, scarce information is available on the charged particles from the ^{7}He decay, precluding its isotopic identification. On the other hand, as discussed in Sec. I, the one-neutron pickup from ^{9}Be should strongly populate the ground state and $1/2^-$state, similar to a (d,p) reaction. In the angular range covered by LEDA, the two-proton pickup may play a role; however, this reaction mechanism does not exclude the population of either the $1/2^-$ or $5/2^-$states. The two-proton pickup reaction at much higher energy has been studied in Ref. [3]. In that case, the populated state at 2.95(10) MeV, shown in Fig. 1, has been interpreted as $5/2^-$ for its agreement with a previously observed resonance [13]. Although further investigation of one-neutron and two-proton pickup contributions would be interesting, the difficulties in describing the latter mechanism, the angular range covered by both detectors, and the limited resolution of the Lamp detector make an assignment of the spin from angular distributions not reliable. Excitation energies and widths from several theoretical calculations are shown in Fig. 1. The properties of the observed resonance are fairly consistent with the results of the resonating group method [16], Green's function Monte Carlo [17] with the AV18/IL2 Hamiltonian, and the continuum shell model [18]. Both the no-core shell model with continuum (NCSMC) [21] and the complex scaling method [20] predict a broad first-excited state but at lower energy with respect to the position indicated in this paper.

In a recent study of π^--induced reactions, Gurov *et al.* [15] set an upper limit of 0.5 MeV on the widths for the first three excited states of ^{7}He. According to our data, a resonance with such Γ_{FWHM} gives a χ^2 higher than 300; thus, it can be excluded at 99% confidence level (CL). The present results are obtained by introducing a minimum number of ^{7}He resonances to describe our spectra. Nevertheless, the presence of more excited states cannot be ruled out. To evaluate an upper limit for the population of a low-lying excited state as that reported in Ref. [4], we performed the fit of the center-of-mass energy of the $^6\mathrm{He} + n$ system in Fig. 8 including such a contribution. This has been simulated according to an R-matrix shape with $E_r = 0.6$ MeV and $\Gamma = 0.75$ MeV. A ratio between the contribution of such a resonance and the ground state larger than 4% can be rejected at 99% CL. Note that such a ratio was 54(1)% in Ref. [4]. The upper limit is further reduced to 3.4% when considering the level claimed in Ref. [6].

V. CONCLUSION

In summary, we have reconstructed the center-of-mass energy of the $^6\mathrm{He} + n$ system with the resonant particle spectroscopy technique to study the unbound nucleus ^{7}He. The method based on the identification of α particles from $^8\mathrm{Be}_{\mathrm{g.s.}}$ decay has been successfully tested with the $^9\mathrm{Be}(^6\mathrm{Li},^7\mathrm{Li})^8\mathrm{Be}$ reaction. The analysis of ^{7}He spectra clearly shows the ground-state resonance, for which properties agree with the previous experiments and the extracted neutron spectroscopic factor is in good accord with the recent *ab initio* calculations. The ^{7}He spectra also suggest a broad resonance at 2.6 MeV. The width and the position of this resonance are significantly consistent with the state populated in a $^6\mathrm{He}(d,p)$ reaction [11]. Although the limited decay information for this resonance requires further investigations, our results are encouraging to finally settle the long-standing puzzle of the ^{7}He first-excited state.

ACKNOWLEDGMENTS

This work has been funded by FWO-Vlaanderen (Belgium) and by the Interuniversity Attraction Poles Programme initiated by the Belgian Science Policy Office (BELSPO) (BriX network P7/12).

[1] R. H. Stokes and P. G. Young, Phys. Rev. Lett. **18**, 611 (1967).
[2] R. H. Stokes and P. G. Young, Phys. Rev. **178**, 2024 (1969).
[3] H. G. Bohlen, R. Kalpakchieva, A. Blažević, B. Gebauer, T. N. Massey, W. von Oertzen, and S. Thummerer, Phys. Rev. C **64**, 024312 (2001).
[4] M. Meister, K. Markenroth, D. Aleksandrov, T. Aumann, L. Axelsson, T. Baumann, M. J. G. Borge, L. V. Chulkov, W. Dostal, B. Eberlein, T. W. Elze, H. Emling, C. Forssén, H. Geissel, M. Hellström, R. Holzmann, B. Jonson, J. V. Kratz, R. Kulessa, Y. Leifels, A. Leistenschneider, I. Mukha, G. Münzenberg,

F. Nickel, T. Nilsson, G. Nyman, A. Richter, K. Riisager, C. Scheidenberger, G. Schrieder, H. Simon, O. Tengblad, and M. V. Zhukov, Phys. Rev. Lett. **88**, 102501 (2002).

[5] G. V. Rogachev, P. Boutachkov, A. Aprahamian, F. D. Becchetti, J. P. Bychowski, Y. Chen, G. Chubarian, P. A. DeYoung, V. Z. Goldberg, J. J. Kolata, L. O. Lamm, G. F. Peaslee, M. Quinn, B. B. Skorodumov, and A. Wöhr, Phys. Rev. Lett. **92**, 232502 (2004).

[6] F. Skaza, V. Lapoux, N. Keeley, N. Alamanos, E. C. Pollacco, F. Auger, A. Drouart, A. Gillibert, D. Beaumel, E. Becheva, Y. Blumenfeld, F. Delaunay, L. Giot, K. W. Kemper, L. Nalpas, A. Obertelli, A. Pakou, R. Raabe, P. Roussel-Chomaz, J.-L. Sida, J.-A. Scarpaci, S. Stepantsov, and R. Wolski, Phys. Rev. C **73**, 044301 (2006).

[7] N. Ryezayeva, C. Bäumer, A. van den Berg, L. Chulkov, D. Frekers, D. D. Frenne, E.-W. Grewe, P. Haefner, E. Jacobs, H. Johanson, Y. Kalmykov, A. Negret, P. von Neumann-Cosel, L. Popescu, S. Rakers, A. Richter, G. Schrieder, A. Shevchenko, H. Simon, and H. Wörtche, Phys. Lett. B **639**, 623 (2006).

[8] D. H. Denby, P. A. DeYoung, T. Baumann, D. Bazin, E. Breitbach, J. Brown, N. Frank, A. Gade, C. C. Hall, J. Hinnefeld, C. R. Hoffman, R. Howes, R. A. Jenson, B. Luther, S. M. Mosby, C. W. Olson, W. A. Peters, A. Schiller, A. Spyrou, and M. Thoennessen, Phys. Rev. C **78**, 044303 (2008).

[9] Y. Aksyutina, H. Johansson, T. Aumann, K. Boretzky, M. Borge, A. Chatillon, L. Chulkov, D. Cortina-Gil, U. D. Pramanik, H. Emling, C. Forssén, H. Fynbo, H. Geissel, G. Ickert, B. Jonson, R. Kulessa, C. Langer, M. Lantz, T. LeBleis, A. Lindahl, K. Mahata, M. Meister, G. Münzenberg, T. Nilsson, G. Nyman, R. Palit, S. Paschalis, W. Prokopowicz, R. Reifarth, A. Richter, K. Riisager, G. Schrieder, H. Simon, K. Sümmerer, O. Tengblad, H. Weick, and M. Zhukov, Phys. Lett. B **679**, 191 (2009).

[10] Z. Cao, Y. Ye, J. Xiao, L. Lv, D. Jiang, T. Zheng, H. Hua, Z. Li, X. Li, Y. Ge, J. Lou, R. Qiao, Q. Li, H. You, R. Chen, D. Pang, H. Sakurai, H. Otsu, M. Nishimura, S. Sakaguchi, H. Baba, Y. Togano, K. Yoneda, C. Li, S. Wang, H. Wang, K. Li, T. Nakamura, Y. Nakayama, Y. Kondo, S. Deguchi, Y. Satou, and K. Tshoo, Phys. Lett. B **707**, 46 (2012).

[11] A. H. Wuosmaa, K. E. Rehm, J. P. Greene, D. J. Henderson, R. V. F. Janssens, C. L. Jiang, L. Jisonna, E. F. Moore, R. C. Pardo, M. Paul, D. Peterson, S. C. Pieper, G. Savard, J. P. Schiffer, R. E. Segel, S. Sinha, X. Tang, and R. B. Wiringa, Phys. Rev. C **72**, 061301 (2005).

[12] A. H. Wuosmaa, J. P. Schiffer, K. E. Rehm, J. P. Greene, D. J. Henderson, R. V. F. Janssens, C. L. Jiang, L. Jisonna, J. C. Lighthall, S. T. Marley, E. F. Moore, R. C. Pardo, N. Patel, M. Paul, D. Peterson, S. C. Pieper, G. Savard, R. E. Segel, R. H. Siemssen, X. D. Tang, and R. B. Wiringa, Phys. Rev. C **78**, 041302 (2008).

[13] A. A. Korsheninnikov, M. S. Golovkov, A. Ozawa, E. A. Kuzmin, E. Y. Nikolskii, K. Yoshida, B. G. Novatskii, A. A. Ogloblin, I. Tanihata, Z. Fulop, K. Kusaka, K. Morimoto, H. Otsu, H. Petrascu, and F. Tokanai, Phys. Rev. Lett. **82**, 3581 (1999).

[14] P. Boutachkov, G. V. Rogachev, V. Z. Goldberg, A. Aprahamian, F. D. Becchetti, J. P. Bychowski, Y. Chen, G. Chubarian, P. A. DeYoung, J. J. Kolata, L. O. Lamm, G. F. Peaslee, M. Quinn, B. B. Skorodumov, and A. Wöhr, Phys. Rev. Lett. **95**, 132502 (2005).

[15] Y. B. Gurov, L. Y. Korotkova, S. V. Lapushkin, R. V. Pritula, V. G. Sandukovsky, M. V. Tel'kushev, and B. A. Chernyshev, JETP Lett. **101**, 69 (2015).

[16] J. Wurzer and H. M. Hofmann, Phys. Rev. C **55**, 688 (1997).

[17] S. C. Pieper, R. B. Wiringa, and J. Carlson, Phys. Rev. C **70**, 054325 (2004).

[18] A. Volya and V. Zelevinsky, Phys. Rev. Lett. **94**, 052501 (2005).

[19] L. Canton, K. Amos, S. Karataglidis, G. Pisent, J. Svenne, and D. van der Knijff, Nucl. Phys. A **790**, 251c (2007).

[20] T. Myo, R. Ando, and K. Katō, Phys. Rev. C **80**, 014315 (2009).

[21] S. Baroni, P. Navrátil, and S. Quaglioni, Phys. Rev. Lett. **110**, 022505 (2013).

[22] D. Tilley, J. Kelley, J. Godwin, D. Millener, J. Purcell, C. Sheu, and H. Weller, Nucl. Phys. A **745**, 155 (2004).

[23] A. Adahchour and P. Descouvemont, Phys. Lett. B **639**, 447 (2006).

[24] S. Baroni, P. Navrátil, and S. Quaglioni, Phys. Rev. C **87**, 034326 (2013).

[25] I. Brida, S. C. Pieper, and R. B. Wiringa, Phys. Rev. C **84**, 024319 (2011).

[26] J. Kelley, E. Kwan, J. Purcell, C. Sheu, and H. Weller, Nucl. Phys. A **880**, 88 (2012).

[27] G. J. Wozniak, N. A. Jelley, and J. Cerny, Phys. Rev. Lett. **31**, 607 (1973).

[28] G. Wozniak, N. Jelley, and J. Cerny, Nucl. Instrum. Methods **120**, 29 (1974).

[29] G. J. Wozniak, D. P. Stahel, J. Cerny, and N. A. Jelley, Phys. Rev. C **14**, 815 (1976).

[30] J. M. Allmond, A. E. Stuchbery, J. R. Beene, A. Galindo-Uribarri, J. F. Liang, E. Padilla-Rodal, D. C. Radford, R. L. Varner, A. Ayres, J. C. Batchelder, A. Bey, C. R. Bingham, M. E. Howard, K. L. Jones, B. Manning, P. E. Mueller, C. D. Nesaraja, S. D. Pain, W. A. Peters, A. Ratkiewicz, K. T. Schmitt, D. Shapira, M. S. Smith, N. J. Stone, D. W. Stracener, and C.-H. Yu, Phys. Rev. Lett. **112**, 172701 (2014).

[31] M. Milin, D. Miljanić, M. Aliotta, S. Cherubini, T. Davinson, A. Di Pietro, P. Figuera, A. Musumarra, A. Ninane, A. N. Ostrowski, M. G. Pellegriti, A. C. Shotter, N. Soić, C. Spitaleri, and M. Zadro, Phys. Rev. C **70**, 044603 (2004).

[32] W. D. M. Rae, A. J. Cole, B. G. Harvey, and R. G. Stokstad, Phys. Rev. C **30**, 158 (1984).

[33] G. Ryckewaert, J. Colson, M. Gaelens, M. Loiselet, and N. Postiau, Nucl. Phys. A **701**, 323 (2002).

[34] M. Loiselet, G. Berger, D. Breyne, Th. Daras, H. Goffaux, N. Postiau, G. Ryckewaert, and J. Ryckewaert, *Proceedings of the 14th International Conference on Cyclotrons and their Applications (CYCLOTRONS 95), Faure, Cape Town, South Africa, 8–13 Oct 1995*, edited J. C. Cornell (World Scientific, Singapore, 1996), p. 629.

[35] T. Davinson, W. Bradfield-Smith, S. Cherubini, A. DiPietro, W. Galster, A. Laird, P. Leleux, A. Ninane, A. Ostrowski, A. Shotter, J. Vervier, and P. Woods, Nucl. Instrum. Methods Phys. Res., Sect. A **454**, 350 (2000).

[36] M. Majer, R. Raabe, M. Milin, C. Angulo, J. Cabrera, E. Casarejos, J. L. Charvet, D. Escrig, A. Gillibert, T. Keutgen, V. Lapoux, L. Nalpas, A. Ninane, A. Obertelli, N. A. Orr, F. Skaza, J. L. Sida, S. I. Sidorchuk, D. Smirnov, and R. Wolski, Eur. Phys. J. A **43**, 153 (2010).

[37] R. J. de Meijer and R. Kamermans, Rev. Mod. Phys. **57**, 147 (1985).

[38] J. Ziegler, *The Stopping and Ranges of Ions in Matter* (Elsevier Science, Burlington, 2013).
[39] S. Agostinelli, J. Allison, K. Amako, J. Apostolakis, H. Araujo, P. Arce, M. Asai, D. Axen, S. Banerjee, G. Barrand, F. Behner, L. Bellagamba, J. Boudreau, L. Broglia, A. Brunengo, H. Burkhardt, S. Chauvie, J. Chuma, R. Chytracek, G. Cooperman, G. Cosmo, P. Degtyarenko, A. Dell'Acqua, G. Depaola, D. Dietrich, R. Enami, A. Feliciello, C. Ferguson, H. Fesefeldt, G. Folger, F. Foppiano, A. Forti, S. Garelli, S. Giani, R. Giannitrapani, D. Gibin, J. G. Cadenas, I. González, G. G. Abril, G. Greeniaus, W. Greiner, V. Grichine, A. Grossheim, S. Guatelli, P. Gumplinger, R. Hamatsu, K. Hashimoto, H. Hasui, A. Heikkinen, A. Howard, V. Ivanchenko, A. Johnson, F. Jones, J. Kallenbach, N. Kanaya, M. Kawabata, Y. Kawabata, M. Kawaguti, S. Kelner, P. Kent, A. Kimura, T. Kodama, R. Kokoulin, M. Kossov, H. Kurashige, E. Lamanna, T. Lampén, V. Lara, V. Lefebure, F. Lei, M. Liendl, W. Lockman, F. Longo, S. Magni, M. Maire, E. Medernach, K. Minamimoto, P. M. de Freitas, Y. Morita, K. Murakami, M. Nagamatu, R. Nartallo, P. Nieminen, T. Nishimura, K. Ohtsubo, M. Okamura, S. O'Neale, Y. Oohata, K. Paech, J. Perl, A. Pfeiffer, M. Pia, F. Ranjard, A. Rybin, S. Sadilov, E. D. Salvo, G. Santin, T. Sasaki, N. Savvas, Y. Sawada, S. Scherer, S. Sei, V. Sirotenko, D. Smith, N. Starkov, H. Stoecker, J. Sulkimo, M. Takahata, S. Tanaka, E. Tcherniaev, E. S. Tehrani, M. Tropeano, P. Truscott, H. Uno, L. Urban, P. Urban, M. Verderi, A. Walkden, W. Wander, H. Weber, J. Wellisch, T. Wenaus, D. Williams, D. Wright, T. Yamada, H. Yoshida, and D. Zschiesche, Nucl. Instrum. Methods Phys. Res., Sect. A **506**, 250 (2003).
[40] A. M. Lane and R. G. Thomas, Rev. Mod. Phys. **30**, 257 (1958).
[41] P. Descouvemont and D. Baye, Rep. Prog. Phys. **73**, 036301 (2010).
[42] O. Kirsebom, Ph.D. thesis, University of Arrhus, 2010 (unpublished).
[43] T. N. D. E. Project, " Energy level diagram, 7li." .
[44] E. W. Hamburger and J. R. Cameron, Phys. Rev. **117**, 781 (1960).
[45] F. Beck, D. Frekers, P. von Neumann-Cosel, A. Richter, N. Ryezayeva, and I. Thompson, Phys. Lett. B **645**, 128 (2007).
[46] A. Bohr and B. Mottelson, *Nuclear Structure* (World Scientific, Singapore, 1969), Vol. 1.
[47] B. K. Jennings, arXiv:1102.3721.
[48] G. D. Westin and J. L. Adams, Phys. Rev. C **4**, 363 (1971).